Interference Analysis of Directional UAV Networks: A Stochastic Geometry Approach

Eunmi Chu
Chungnam National University
Daejeon, South Korea, 34134
E-mail: emchu@cnu.ac.kr

Jong Min Kim
Korea Science Academy of KAIST
Busan, South Korea, 47162
E-mail: franzkim@gmail.com

Bang Chul Jung
Chungnam National University
Daejeon, South Korea, 34134
E-mail: bcjung@cnu.ac.kr

***Abstract*—We characterize the interference characteristics of directional unmanned aerial vehicle (UAV) networks based on the stochastic geometry, where each UAV is equipped with a directional antenna and is placed in three dimensional (3D) locations. In particular, the 3D location of UAVs is assumed to be uniformly distributed in a certain volume, which is modeled by Poisson point process. Given a beamwidth, we first design an ideal 3D directional antenna model with a constant gain of both main-lobe and side-lobe. Then, we investigate the aggregate interference at a typical UAV receiver from multiple UAVs. Extensive simulation results show that the aggregate interference becomes significantly decreased if the beamwidth decreases or the antenna gain of side-lobe decreases.**

***Keywords*—UAV networks, Poisson point process (PPP), 3D directional antenna, interference, stochastic geometry.**

I. Introduction

Recently, an unmanned aerial vehicles (UAV) communication has widely been investigated with various applications due to its low cost of deployment and rapid stabilization of networks. In general, the UAV applications include real-time monitoring of road traffic, remote sensing, disaster communications, product delivery, precision agriculture, etc [1]. Most studies on the UAV communication have focused on performance improvement for terrestrial wireless networks. A framework of UAV-assisted vehicular network was introduced in [2], where it was shown that various performance metrics such as vehicle-to-vehicle connectivity, infrastructure coverage, network information collection ability, and network interworking efficiency can be improved by cooperating the UAVs and terrestrial communication infrastructure. In [3], coverage probability at a ground user in the UAV-assisted network where multiple UAVs are assumed to located in a three-dimensional (3D) space and they are assumed to move based on the mixed random waypoint mobility model. In [4], a cooperative data dissemination framework was proposed in air-ground integrated networks to maximize the minimum received data amount of ground users, where a terrestrial base station and a single UAV cooperatively serve ground users.

Different from UAV-assisted terrestrial wireless networks, a communication among UAVs has not received much attention from both academia and industry due to relatively rare applications and hash technical challenges such as highly mobility of UAVs and frequent topology changes. However, a network consisting of multiple UAVs which are connected by air-to-air wireless channels has recently been investigated due to the increase in the deployment of UAVs. In [5], a novel directional medium access control (MAC) protocol was proposed to coordinate transmissions of many UAVs, equipped with directional antennas, in 3D space. Furthermore, an mmWave-enabled UAV swarm network was studied for massive data exchange among UAVs in [6], where a 3D interference graph was exploited by considering mobility, interference, and energy consumption simultaneously.

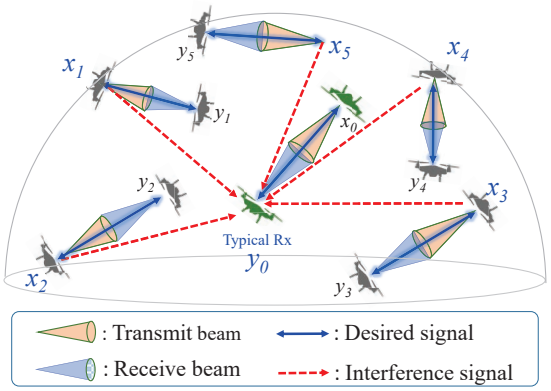

Fig. 1. Directional UAV networks

As the UAV network become denser, the interference among UAV wireless links tends to limit the network performance and thus it is important to analyze the interference characteristics of the UAV network in 3D space as shown in Fig. 1. Existing studies only focused on a simple 3D wireless network without considering the effect of side-lobe of the directional antennas. In this paper, we first introduce an ideal 3D directional antenna model considering the effect of side-lobe and then analyze the interference characteristics of the directional UAV network where UAVs are randomly located in 3D space according to Poisson Point Process (PPP).

II. Interference Modeling

A. Directional Antenna Model in 3D Space

In the ideal omni-directional antenna, the radiation pattern is uniformly radiated to the area of the isotropic sphere. When the radius of sphere is set to 1, surface area $\mathcal{A}_o$ is to be 4π. Since the energy source power $\mathcal{P}_o$ is radiated on $\mathcal{A}_o$, radiation

intensity G_o is to be $\frac{\mathcal{P}_o}{\mathcal{A}_0}$. Radiation intensity means the power radiated from an antenna per unit sphere. Assuming that G_o is 1, then $\mathcal{P}_o$ is to be 4π.

In contrast, in the directional antenna, the radiation pattern is consisted of a main-lobe and a side-lobe. The same $\mathcal{P}_o$ as the omni energy source is separated into $\mathcal{P}_m$ and $\mathcal{P}_s$ where $\mathcal{P}_m$ and $\mathcal{P}_s$ denote the radiated energy on the areas of the main-lobe and side-lobe, respectively. Let the surface area of main-lobe and side-lobe with beamwidth ω be $\mathcal{A}_m$ and $\mathcal{A}_s$, respectively. The area sum of $\mathcal{A}_m$ and $\mathcal{A}_s$ is equal to $\mathcal{A}_o$, i.e., 4π. Therefore, $\mathcal{A}_m$ and $\mathcal{A}_s$ are calculated by as follows:

$$\begin{aligned} \mathcal{A}_m(\omega) &= \int_{\rho=0}^{\omega}\int_{\phi=0}^{\omega} \sin\phi \, d\phi \, d\rho, \\ \mathcal{A}_s(\omega) &= \mathcal{A}_o - \mathcal{A}_m(\omega), \end{aligned} \tag{1}$$

where ρ and ϕ denote azimuth and elevation in a spherical coordinate system, respectively.

Simarly, the radiation intensity of main-lobe and side-lobe is expressed as follows:

$$G_m = \frac{\mathcal{P}_m}{\mathcal{A}_m(\omega)}, \quad G_s = \frac{\mathcal{P}_s}{\mathcal{A}_s(\omega)} = \frac{\mathcal{P}_o - \mathcal{P}_m}{\mathcal{A}_o - \mathcal{A}_m(\omega)}. \tag{2}$$

The energy source power is calculated by

$$\mathcal{P}_m = \mathcal{P}_o - G_s\left(\mathcal{A}_o - \mathcal{A}_m(\omega)\right). \tag{3}$$

The gain of directional antenna is defined as the ratio of the radiation intensity of directional antenna to that of omni-directional antenna. Since G_o is 1, the antenna gain of main-lobe is G_m and the antenna gain of main-lobe is G_s, respectively. Therefore, given ω and G_s, the gain of main-lobe is derived as follows:

$$G_m = \frac{4\pi - G_s\left(\mathcal{A}_o - \mathcal{A}_m(\omega)\right)}{\mathcal{A}_m(\omega)}. \tag{4}$$

B. Network Model in 3D Space

We consider a 3-dimensional UAV networks where simultaneously transmitting nodes (i.e., UAVs) are distributed as PPP $\Phi = \{x_1, x_2, \cdots\}$ on $\mathbb{R}^3$ of intensity λ ($\mathcal{C}1$). We present y_i as a receiving node corresponding to x_i. We assume that the pair of x_i and y_i is perfectly aligned toward the center direction of beamwidth ω as well as the distance between x_i and y_i is retained with the distance of R ($\mathcal{C}2$). The value on z-axis of x_i, i.e., the height of UAV h_{xi} must be between the minimum of height h_{min} and the maximum of height h_{max}, ($\mathcal{C}3$). In summary, x_i and y_i are randomly and uniformly generated along with the following constraints:

$$\begin{aligned} &\mathcal{C}1: x_i = (a_{xi}, b_{xi}, h_{xi}),\ y_i = (a_{yi}, b_{yi}, h_{yi}) \text{ on } \mathbb{R}^3, \\ &\mathcal{C}2: \|x_i - y_i\| = R, \\ &\mathcal{C}3: h_{min} \le h_{xi}, h_{yi} \le h_{max}. \end{aligned}$$

A typical receiver y_o is located in the center of an observing target area, and the pair of x_o and y_o also retains the distance R. To easily calculate antenna gain, we translate the cartesian coordinate system into the spherical coordinate system. Elevation ϕ is the angle between the vector of r and the z-axis whereas azimuth ρ is the angle between x-axis and the projection of the vector r on the xy plane as shown in Fig. 2. The angles $(\rho_{x_{io}}, \phi_{x_{io}})$ and $(\rho_{x_{oi}}, \phi_{x_{oi}})$ are generated by

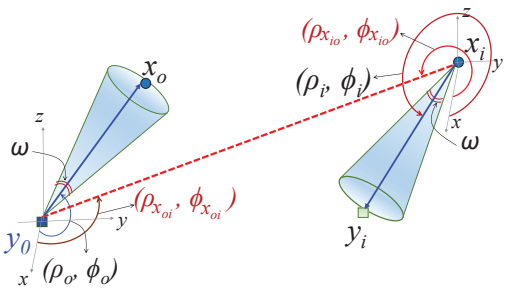

Fig. 2. UAV's antenna gain model

a vector of $(x_i,\ y_o)$ and a vector of $(y_o,\ x_i)$, respectively. Likewise, the angles (ρ_o, ϕ_o) and (ρ_i, ϕ_i) are generated by their pairs, i.e., a vector of $(y_o,\ x_o)$ and a vector of $(x_i,\ y_i)$.

Transmit antenna gain at the typical node x_o from interference node x_i is expressed as follows:

$$\begin{aligned} &\mathcal{G}_t\left(\rho_{x_{io}}, \phi_{x_{io}}, \omega\right) \\ &\quad = \begin{cases} G_m, \text{if } \left(\rho_{x_{io}} \in \overrightarrow{\Psi}_i\right) \cap \left(\phi_{x_{io}} \in \overrightarrow{\Phi}_i\right), \\ G_s, \text{otherwise}, \end{cases} \end{aligned} \tag{5}$$

where $\overrightarrow{\Psi}_i$ and $\overrightarrow{\Phi}_i$ denote angle of main-lobe for a pair of x_i and y_i, i.e., $\overrightarrow{\Psi}_i = \left(\rho_i - \frac{\omega}{2}, \rho_i + \frac{\omega}{2}\right)$ and $\overrightarrow{\Phi}_i = \left(\phi_i - \frac{\omega}{2}, \phi_i + \frac{\omega}{2}\right)$.

Receiver antenna gain at the typical node y_o from interference node x_i is expressed as follws:

$$\begin{aligned} &\mathcal{G}_r\left(\rho_{x_{oi}}, \phi_{x_{oi}}, \omega\right) \\ &\quad = \begin{cases} G_m, \text{if } \left(\rho_{x_{oi}} \in \overleftarrow{\Psi}_i\right) \cap \left(\phi_{x_{oi}} \in \overleftarrow{\Phi}_i\right), \\ G_s, \text{otherwise}, \end{cases} \end{aligned} \tag{6}$$

where $\overleftarrow{\Psi}_i$ and $\overleftarrow{\Phi}_i$ denote angle of main-lobe for a pair of x_o and y_o, i.e., $\overleftarrow{\Psi}_i = \left(\rho_o - \frac{\omega}{2}, \rho_o + \frac{\omega}{2}\right)$ and $\overleftarrow{\Phi}_i = \left(\phi_o - \frac{\omega}{2}, \phi_o + \frac{\omega}{2}\right)$.

Therefore, the received desired signal $\mathcal{S}$ and the interference signal I at the typical receiver y_o are expressed as follows:

$$\begin{aligned} \mathcal{S} &= P_t R^{-\alpha} G_m G_m, \\ I &= \sum_{i \in \Phi} P_t d_i^{-\alpha} \mathcal{G}_t\left(\rho_{x_{oi}}, \phi_{x_{oi}}, \omega\right) \mathcal{G}_r\left(\rho_{x_{oi}}, \phi_{x_{oi}}, \omega\right), \end{aligned} \tag{7}$$

where P_t denotes transmit power, and d_i denotes the distance between interference nodes and the typical receiver, i.e., $d_i = \|x_i - y_o\|$. Then, SINR is given by $\frac{\mathcal{S}}{I+\eta}$ where η denotes noise power.

III. Simulation Results

System parameters are set to $R = 100\,\text{m}$, $\alpha = 2^*$, service area $A = 10\,\text{km} \times 10\,\text{km}$, $\lambda A = 100 \sim 500$ nodes, and $\omega = \{10°, 30°, 60°, 120°\}$, and $G_s = 0 \sim 0.2$.

Fig. 3 shows the effect of G_m for varying G_s and ω in dB scale units. Fig. 4 shows the CDF of aggregate interference according to ω. In case of an omni-directional antenna, aggregate interference is between -48 dB and -25 dB. However,

*The path-loss exponent for air-to-air was also estimated at 2.05 (slightly more than the free space path-loss exponent of 2.0 [7].

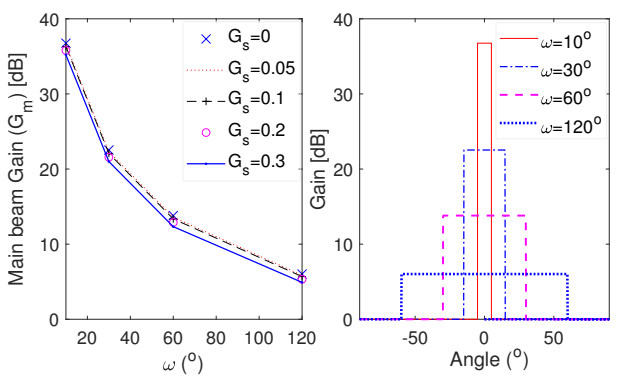

Fig. 3. Antenna gain of main-lobe (G_m) according to beamwidth (ω) and the antenna gain of side-lobe (G_s).

for $\omega = 10°$, aggregate interference is between -70dB and 8dB. Although 70% of aggregate interference is less than -65dB, about 20% cause strong interference greater than -40 dB. Strong interference begins to decrease at $60°$ and there is no overall strong interference at $120°$. Therefore, strong interference cancellation seems to be necessary for the narrow beamwidth.

Fig. 5 shows the CDF of aggregate interference according to the variation of G_s at $\omega = 120°$. For $G_s = 0$, 99% of the nodes cause small interference amount less than -100dB, therefore, As G_s increases, the amount of interference increases due to side-lobe. Fig. 6 shows CDF of SINR according to ω. For small ω, the antenna gain of the main-lobe is large as shown in Fig. 3. From this, it can be seen that the SINR increases due to a sharp increase in the desired signal. In case of $\omega = 10°$, SINR can be seen to increase sharply due to 70% weak interference and the strong desired signal.

IV. Conclusions

In this paper, we considered a large directional UAV network in 3D space where UAVs are randomly located according to PPP. It was shown that the narrower beamwidth increases the signal strength but it may induce strong interference to other UAV wireless links as well. Therefore, interference management techniques are required for the directional UAV network. In addition, the side-lobe significantly affects the interference characteristics. We leave the interference management such as interference avoidance or cancellation for the directional UAV network as a further study.

Acknowledgement

This work was partly supported by the Korea Science Academy of KAIST with funds from the Ministry of Science and ICT and this work was partly supported by the ICT R&D program of MSIT/IITP. (2019-0-00964-001, Development of Incumbent Radio Stations Protection and Frequency sharing Technology through Spectrum Challenge).

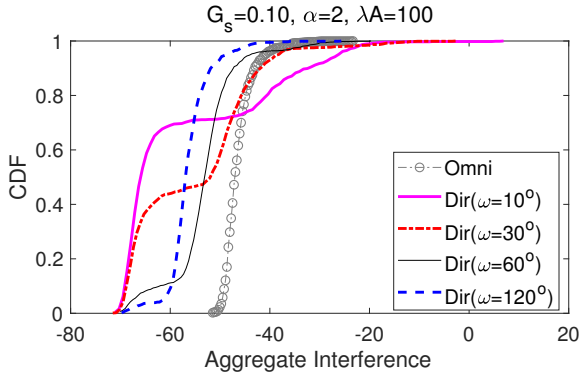

Fig. 4. CDF of the aggregate interference according to ω.

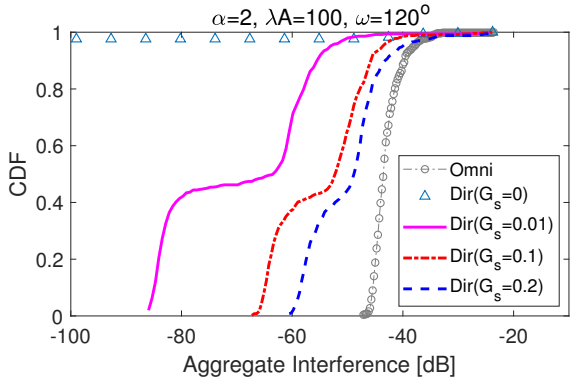

Fig. 5. CDF of the aggregate interference according to G_s.

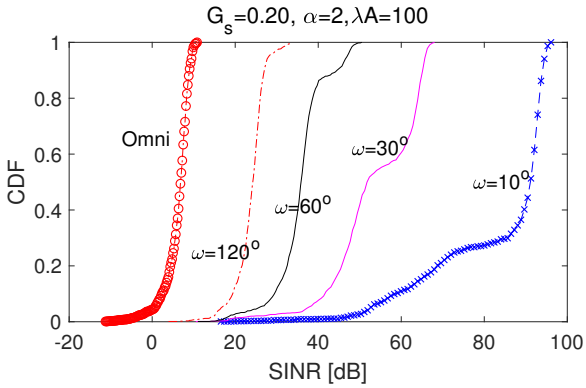

Fig. 6. CDF of SINR according to ω.

References

[1] H. Shakhatreh, *et al.*, "Unmanned aerial vehicles: A survey on civil applications and key research challenges," *arXiv preprint arXiv:1805.00881*, Apr. 2018.

[2] W. Shi, H. Zhou, J. Li, W. Xu, N. Zhang, and X. Shen, "Drone assisted vehicular networks: Architecture, challenges and opportunities," *IEEE Netw.*, vol. 32, no. 3, pp.130–137, May/June 2018.

[3] P. Sharma and D. Kim, "Coverage probability of 3-D mobile UAV networks," *IEEE Wireless Commun. Lett.*, vol. 8, no. 1, pp. 97–100, Feb. 2019.

[4] Z. Xue, J. Wang, and G. Ding, "Cooperative data dissemination in air-ground integrated networks," *IEEE Wireless Commun. Lett.*, vol. 8, no. 1, pp. 209–212, Feb. 2019.

[5] Z. Zheng, A. Sangaiah, and T. Wang, "Adaptive communication protocols in flying ad hoc network," *IEEE Commun. Mag.*, vol. 56, no. 1, pp.136–142, Jan. 2018.
[6] Z. Feng, L. Ji, Q. Zhang, and W. Li, "Spectrum management for mmwave enabled UAV swarm networks: Challenges and opportunities," *IEEE Commun. Mag.*, vol. 57, no. 1, pp.146–153, Jan. 2019.
[7] N. Ahmed, S. Kanhere, and S. Jha, "On the importance of link characterization for aerial wireless sensor networks," *IEEE Commun. Mag.*, vol. 54, no. 5, pp.52–57, May 2016.